Increasing Integration of Wind Power in Medium Voltage Grid by Voltage Support of Smart Transformer

X Gao
G de Carne
M Liserre
Chair of Power Electronics
Christian-Albrechts-Universität zu Kiel
xg@tf.uni-kiel.de

C Vournas
National Technical University of Athens

Abstract. The voltage rise during wind energy penetration represents a limit of the wind power integration in the distribution grid. The Smart Transformer (ST), a power electronics-based transformer, can provide additional services to the distribution grids, for instance the voltage support in MV grid by means of reactive power injection. In this paper, this service is applied to increase the hosting capacity of wind power in MV grids.

Keywords: Wind power integration, smart transformer, voltage support

1. Introduction

The world requires more and more emission free green energy. With the development of generation technology, wind energy becomes an important alternative for fossil energy and nuclear energy. The installed capacity of wind power generators has been increased dramatically in past years worldwide. In EU, the cumulative wind power generators installation in 2015 is 141.6GW, the double of the capacity in 2008 (65.1GW) [1]. The wind energy can be either generated from hundreds MW-scale wind farms or from Distribution Wind Generator (DWG) with capacity up to a few megawatts [2].

The DWG connects usually directly to the distribution grid, where wind energy is available. However, in the installation places, the distribution grid is usually weak and the ratio of resistance to reactance R/X of the line is high [3]. In case of high wind energy production and low load consumption, high voltage rises can occur [3] [4]. If the voltage rise violates the upper voltage constraints, the wind power must be curtailed to ensure the electrical appliances safety in the distribution grid [4].

The methods for ensuring voltage regulation in presence of high integration of DWG are classified into 2 categories. The first one uses the power converters from wind generator itself. For instance, the Doubly-Fed Asynchronous Generator (DFAG) and full converter wind generator can support the voltage by means of reactive power injection [5].

The second category uses external equipment for the voltage control, for instance Static VAr Compensator (SVC), or Transformer with Load Tap-Changer (LTC) [6]-[8]. The SVC supports the voltage by means of reactive power injection. However, the SVC has no ability to isolate the contingency: the SVC cannot avoid the propagation of one contingency from Medium Voltage (MV) to Low Voltage (LV) grid. Transformers equipped with LTC and connected to the High Voltage HV/ MV grids, can adjust the voltage amplitude varying the tap-changer set point. The LTC transformer can adjust the voltage amplitude only with discrete time steps, e.g. minimal change step is 1% [9]. Furthermore, the transformer with LTC is not a flexible control method, because the action of tap-changer changes the voltage profile of the whole MV grid [7].

The power electronics based smart transformer (ST) provides efficient and reliable voltage transformation and bi-direction active power transfer between MV and LV grid similar to the traditional transformer [10] [11]. Furthermore, ST enables control of the voltage amplitude dynamically, and decoupling of the MV and LV grids. With additional controller, the ST is also able to provide ancillary services, e.g. mitigation of harmonics pollution, voltage/current balancing, power factor correction, reactive power injection.

In MV distribution grids, the ST provides a new solution to increase the grid integration of DWGs. This paper studies the ability of voltage support in MV grid by ST in different conditions.

The paper is structured as follows, Section II will introduce the configuration and control strategy of ST, Section III will present the testing model, Case studies will be shown in Section IV and the conclusion and discussion will be given in Section V.

2. Smart transformer concept and control

2.1. ST general configuration

The basic configuration of ST is shown in figure 1. ST has 3 stages, one AC/DC converter at MV side, one DC/DC converter, and one DC/AC converter at LV side. There are 2 DC links at each MV and LV side. The DC links can be used to connect renewable energy sources and battery energy storage systems [10] [11]. Only active power is exchanged between MV and LV grids.

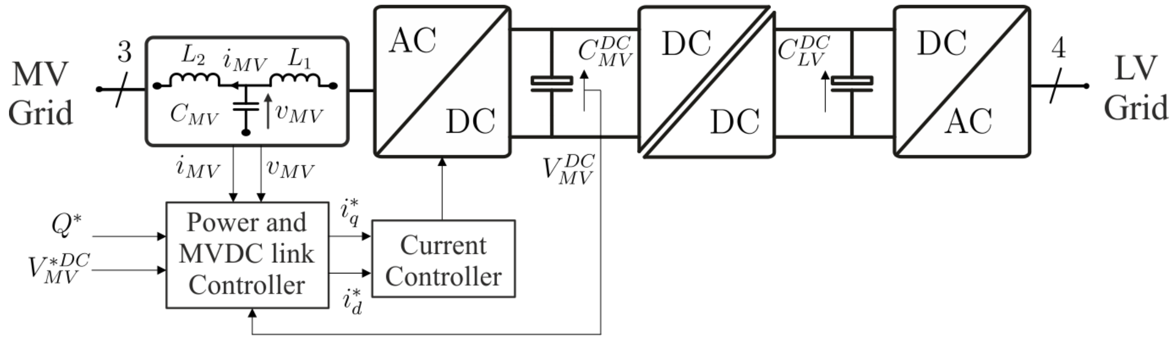

Figure 1: General structure of ST

ST achieves electrical separation of MV and LV grids by means of the MV and LV DC links [10]. The MV and LV converters can be sized independently. Any contingency (e.g. voltage sags, voltage fluctuations) at one side is damped in the other side. The DC/AC inverter imposes a sinusoidal voltage waveform V_{LV} with constant amplitude and frequency independently from the load current absorption. The DC/DC converter enables the active power transfer between the MV and LV grids, and controls the LV DC link voltage. In the MV side, the power/MVDC link controller ensures constant MV DC link voltage, and generates the reference values of i_d^* and i_q^* based on the $V_{MV}^{*\mathrm{DC}}$ (which reflects active power transformation) and Q^* (reference value of reactive power compensation). The two values i_d^* and i_q^* are sent to a current controller that determines the new gates signals to be sent to the AC/DC converter.

2.2. ST reactive power controller

The capacity of ST for reactive power compensation is determined by the size of ST S_{ST} and the active power transfer P_{ST}. The ST constraints in providing reactive power are determined by the equation:

$$Q_{ST,\max} = \pm\sqrt{S_{ST}^2 - P_{ST}^2} \tag{1}$$

Figure 2 shows the droop control implemented for the voltage support: after exceeding the voltage threshold ($U_{A,min}$ $U_{A,max}$), the reactive power compensation function of ST is activated. The amount of reactive power is injected in proportion to the voltage variation. The droop control may be employed to support DWG integration for controlling the voltage in case of high wind turbines penetration, or to sustain the grid in case of fast voltage variations, e.g. voltage sags or swells.

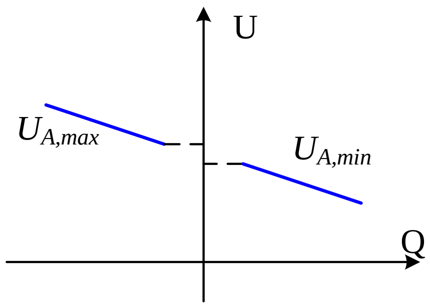

Figure 2. Droop control characteristics for reactive power injection

3. Setup of MV feeder model

In order to check the voltage support capability of the ST in a MV grid, a 20kV feeder with 8 buses is modeled in PSCAD/EMTDC. The structure of the feeder is shown in figure 3. The main grid is 135kV with the short circuit capacity of 1400 MVA. The HV/MV transformer is 132/20 kV with X_T of transformer is 8%. The tap-changer is fixed to 1pu.

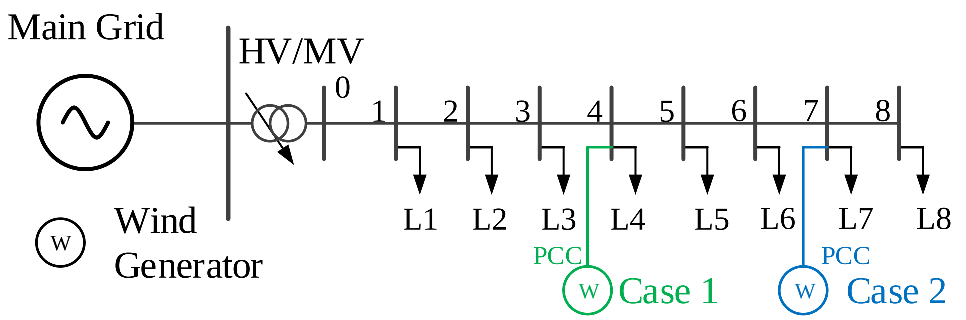

Figure 3. Feeder structure

The parameters of lines are listed in table 1.

Table 1. Impedance of lines

Bus No. 1	Bus No. 2	R (Ω)	X (Ω)
0	1	0.34125	0.480
1	2	0.34125	0.480
2	3	0.34125	0.480
3	4	0.34125	0.480
4	5	0.2281	0.3204
5	6	0.2281	0.3204
6	7	0.2281	0.3204
7	8	0.2281	0.3204

Table 2 shows the load amount for the full load condition. As aforementioned, the worst condition is represented by light load and high wind power penetration. Suggested in [12], the light load case is 25% of the load amount shown in Table 2.

Table 2. Load condition at the heaviest load case

Load No.	P (kW)	Q (kVar)
L1	313	153
L2	313	153
L3	272.5	133.35
L4	272.5	133.35
L5	1368.5	669
L6	1368.5	669
L7	2458	1201.85
L8	2458	1201.85

The DWG model is implemented in the software as Doubly Fed Asynchronous Generator (DFAG). The model of DFAG presented in [13] [14] is used. DFAG uses an ideal step-up transformer to connect with feeder. The power factor of DWG at the Point of Common Coupling (PCC) is kept to the unity.

Two DWG connection scenarios have been considered: connected to close to main grid, i.e. Bus 4 (Case 1) or far away from the main grid, i.e. Bus 7 (Case 2), as shown in figure 4. The short-circuit capacity of Bus 4 is 88.56 MVA, and it of Bus 7 is 60.85 MVA. During the penetration of wind energy, the control aim is to keep voltage from Bus 1 to Bus 8 within (0.975, 1.025).

The size of ST at MV side is 1MVA. In order to investigate the ST performances, it has been assumed that the ST can inject reactive power within its size constraints. For both cases, the ST is connected to Bus 4 as in figure 4.

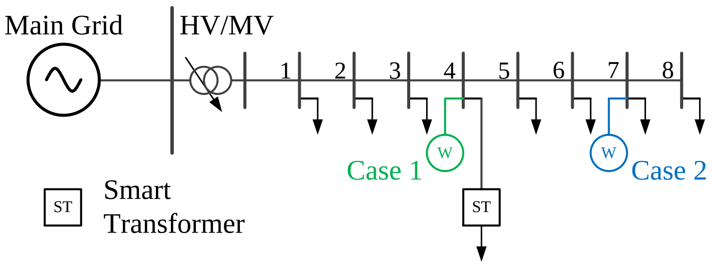

Figure 4. Feeder configuration with ST

4. Case studies

In order to validate the effectiveness of the proposed strategy, the simulation results for two cases are shown as follows. To analyse the voltage variations during penetration of wind energy, for both cases, the voltage amplitudes of all buses are observed. The DWG is assumed to generate active power of its maximal ability. The hosting capacity is the maximal size of DWG which does not lead any bus voltage exceeding the range of voltage i.e. (0.975, 1.025) in pu.

4.1. Case 1

The first case takes in account a grid without ST implementation, indicated as 'Case 1' in figure 3. The voltage variations of all 8 buses are presented in figure 5 when connected with different size of DWG. It is observed within 6MW of DWG size, the voltage of Bus 4 is lower than 1.025 pu. This result implies that the hosting capacity of wind power in this MV feeder is 6MW when DWG is connected at Bus 4.

Bus 4 has the largest variation of voltage. From Bus 1 to Bus 3, the closer to the main grid is the bus, the less voltage variation has the bus. From Bus 5 to Bus 8, voltages of all 4 buses increase, but those voltages are never higher than Bus 4.

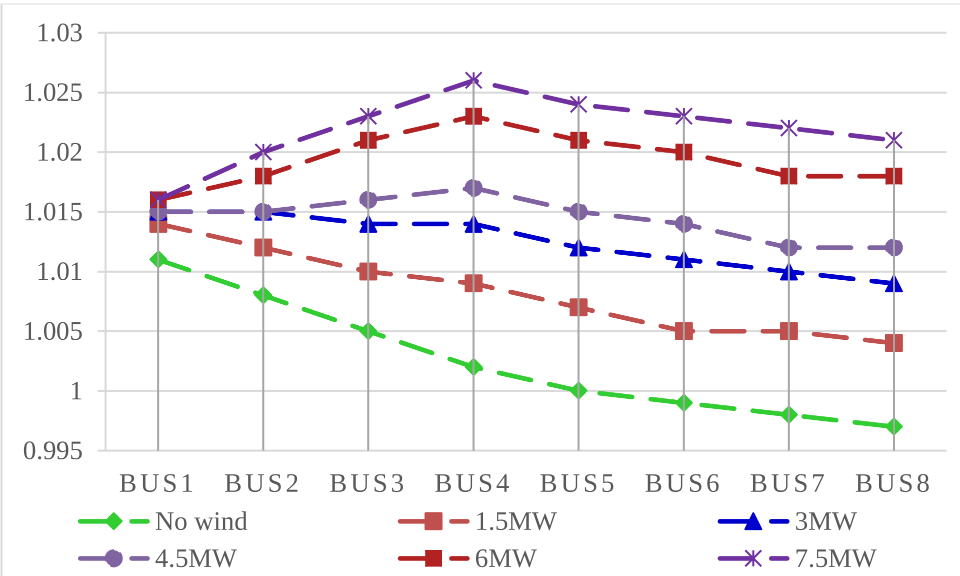

Figure 5. Voltage variation with different capacity of DWG without ST (Case 1)

After ST is connected, the structure of the feeder is shown as 'Case 1' in figure 4. In figure 6, it presents the results from simulation after ST implementation. The bus voltage profile in the feeder does not exceed the upper voltage limit until the size of DWG reaches 13.5MW. The hosting capacity of wind power has been increase to 12MW.

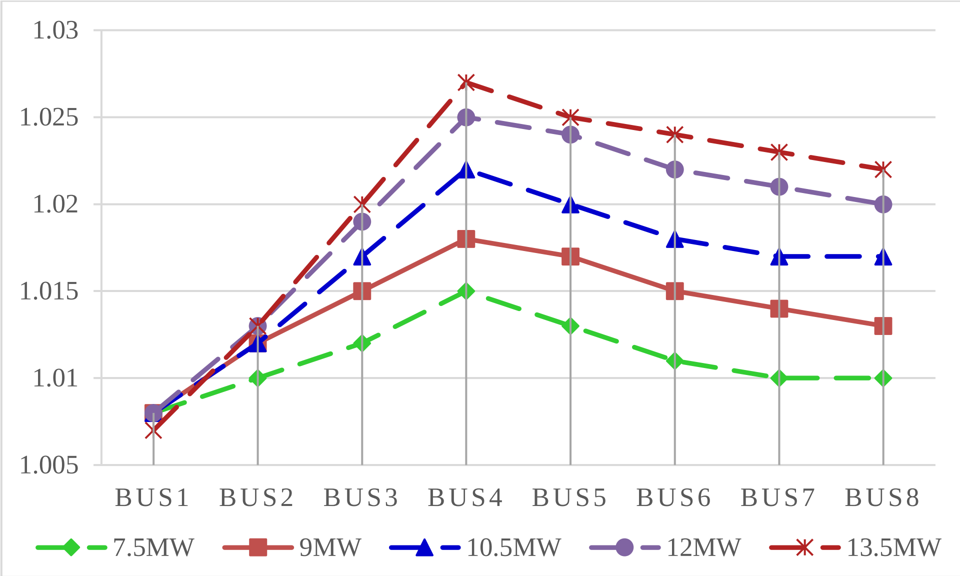

Figure 6. Voltage variation with different capacity of DWG with ST (Case 1)

4.2. Case 2

Figure 7 shows the voltage profile with different sizes of DWG at Bus 7 when there is no ST. The hosting capacity of the grid results to be 4.5MW in order to not violate the upper voltage limit.

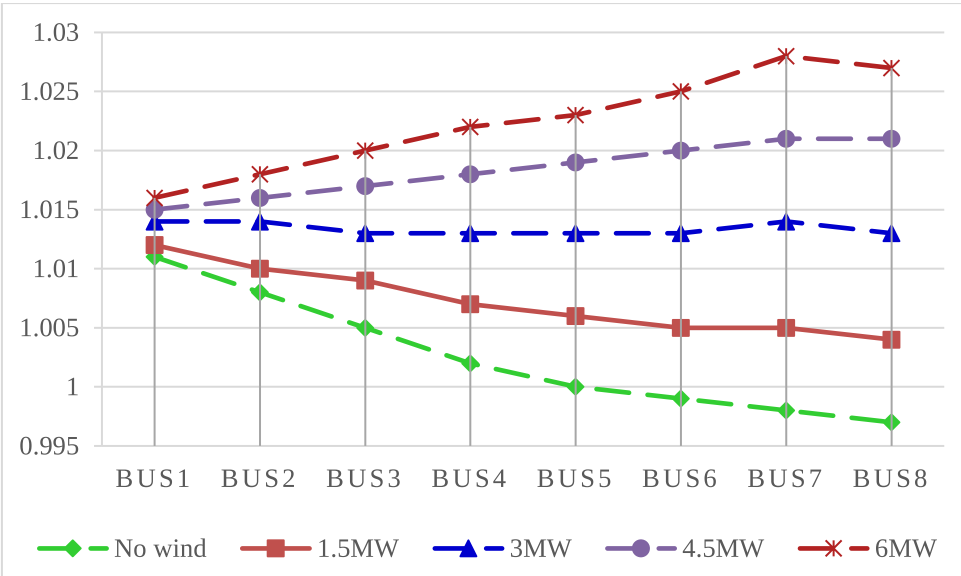

Figure 7. Voltage variation with different capacity of DWG without ST (Case 2)

Bus 7 has the largest variation of voltage. From Bus 1 to Bus 6, the closer to DWG (Bus 7) is the bus, the larger voltage variation has it.

Connecting the ST at Bus 4, the hosting capacity increases to 7.5MW, as shown in Fig. 8.

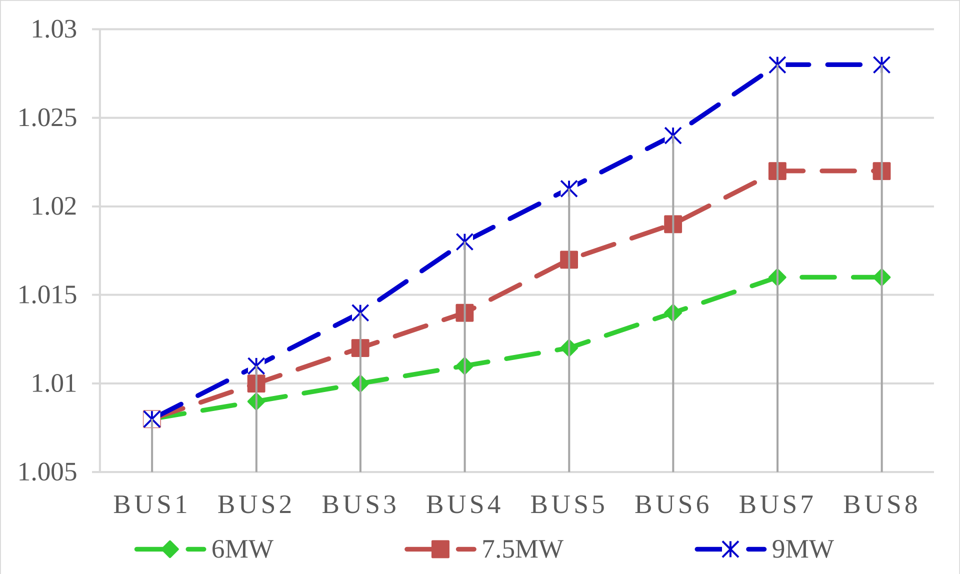

Figure 8. Voltage variation with different capacity of DWG with ST (Case 2)

Concluding, the ST can increase the hosting capacity of wind power in the testing feeder, for both cases when the DWG is close to main grid and when it is at the end of the feeder. As shown in figure 9, if the DWG is close to main grid, the hosting capacity increases by 100%; instead in Case 2, the hosting capacity increase results limited at 67%.

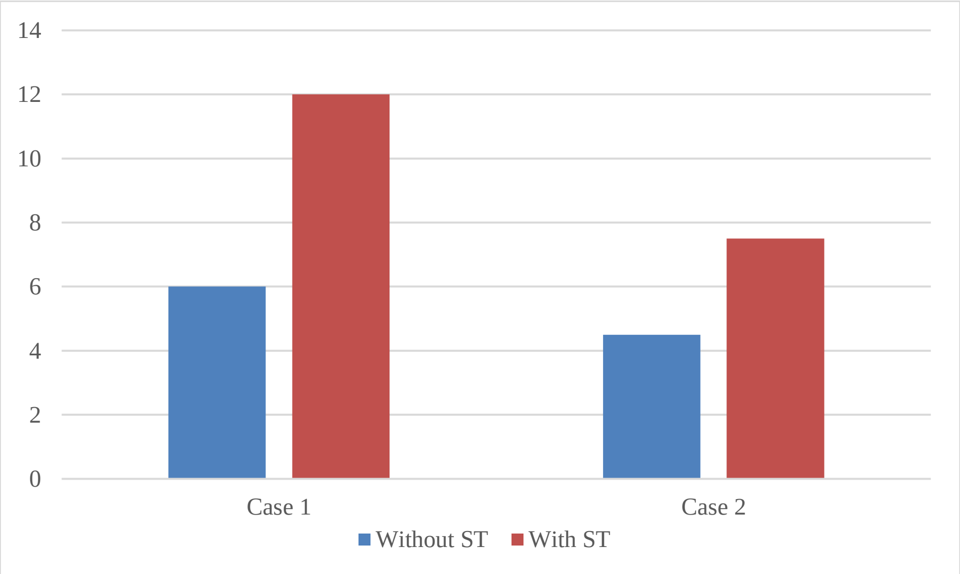

Figure 9. Maximal capacity of wind generation to be connected

5. Conclusions

Voltage rise during the penetration of wind energy limits the hosting capacity of wind power in a distribution grid. In MV distribution grids, ST can effectively provide voltage support to counter voltage rise by means of the reactive power injection.

This paper has analysed the ST voltage support service in a MV distribution grid. The ST feature to increase the wind power integration capability is studied in PSCAD/EMTDC, simulated in an 8-bus MV feeder. Cases where the DWG is close to main grid and at the end of the feeder are considered. The voltage profiles for both cases with different size of wind power, without and with ST are obtained through simulation.

The results of the simulation show how the ST reactive power injection increases more than 60% of the hosting capacity of wind power in the MV feeder.

References

[1] "Wind in power: 2015 European statistics". 2016; 11.

[2] El-Khattam W, Salama M. "Distributed generation technologies, definitions and benefits". *Electric Power*

Systems Research 2004; Vol. 71 Issue 2: 119-128.

[3] Dinic N, Fox B, Flynn D, Xu L. “Increasing wind farm capacity”. *IEE Proceedings - Generation, Transmission and Distribution* 2006; Vol. 153 Issue 4: 493-498.

[4] Liew S. N, Strbac G. M. “Maximising penetration of wind generation in existing distribution networks”. *IEE Proceedings - Generation, Transmission and Distribution* 2002; Vol.149 Issue 3: 256-262.

[5] Carvalho M. S, Correia F, Ferreira A. F. M. “Distributed reactive power generation control for voltage rise mitigation in distribution networks”. *IEEE Transactions on Power Systems* 2008; Vol.23 Issue 2: 766-772.

[6] Gao C, Redfern M. “A review of voltage control techniques of networks with distributed generations using on-load tap changer transformers”. *45th International Universities Power Engineering Conference*; Cardiff, 2010.

[7] De Carne G, Liserre M, Christakou K, Paolone M. “Integrated voltage control and line congestion management in active distribution networks by means of smart transformers”. *IEEE 23rd International Symposium on Industrial Electronics*; Istanbul, 2014: 2613-2619.

[8] Opila D, Arbor A, Zeynu A, Hiskens I. “Wind farm reactive support and voltage control”. *Conference on Bulk Power System Dynamics and Control (iREP) - VIII (iREP)*; Rio de Janeiro, 2010.

[9] Virayavanich S, Seiler A, Hammer C,. Weck K.-H. “Reliability of on-load tap changers with special consideration of experience with delta connected transformer windings and tropical environmental conditions”. *CIGRE-Report*; Paris, 1996.

[10] De Carne G, Buticchi. G, Liserre M, Yoon C, Blaabjerg F. “Voltage and current balancing in low and medium voltage grid by means of smart transformer”. Conference on IEEE Power & Energy Society General Meeting; Denver, 2015.

[11] Kumar C, Liserre M. “A new prospective of smart transformer application: Dual microgrid (DMG) operation”. Conference on IECON 2015 - 41st Annual Conference of the IEEE; Yokohama 2015.

[12] Di Fazio A, Fusco G, Russo M. “Decentralized control of distributed generation for voltage profile optimization in smart feeders”. *IEEE Transactions on Smart Grid* 2013; Vol.4 Issue 3: 1586-1596.

[13] Tsourakis G, Nomikos B.M, Vournas C. “Effect of wind parks with doubly fed asynchronous generators on small-signal stability”. *Electric Power Systems Research* 2009; 79: 190-200.

[14] Cigre Working group 4.601. “Modeling and dynamicbehaviour of wind generation as it relateds to power system control and dynamic performance”. ISBN: 978-2-85873-016-2.